A network approach to investigating the key microbes and stability of gut microbial communities in a mouse neuropathic pain model

Guo-Jie Brandon-Mong
Biodiversity Research Center Academia Sinica
Grace Tzun-Wen Shaw
Biodiversity Research Center Academia Sinica
Wei-Hsin Chen
Institute of Biomedical Sciences Academia Sinica
Chien-Chang Chen
Institute of Biomedical Sciences Academia Sinica
Daryi Wang (dywang@gate.sinica.edu.tw)
Academia Sinica

Research article

Keywords: microbiota, next-generation sequencing, diversity, disturbance, chronic pain, interaction

Posted Date: September 4th, 2020

DOI: https://doi.org/10.21203/rs.3.rs-33943/v2

Version of Record: A version of this preprint was published on September 30th, 2020. See the published version at https://doi.org/10.1186/s12866-020-01981-7.

Abstract

Background: Neuropathic pain is an abnormally increased sensitivity to pain, especially from mechanical or thermal stimuli. To date, the current pharmacological treatments for neuropathic pain are still unsatisfactory. The gut microbiota reportedly plays important roles in inducing neuropathic pain, so probiotics have also been used to treat it. However, the underlying questions around the interactions in and stability of the gut microbiota in a spared nerve injury-induced neuropathic pain model and the key microbes (i.e., the microbes that play critical roles) involved have not been answered. We collected 66 fecal samples over two weeks (three mice and 11 time points in spared nerve injury-induced neuropathic pain and Sham groups). The 16S rRNA gene was polymerase chain reaction amplified, sequenced on a MiSeq platform, and analyzed using a MOTHUR- UPARSE pipeline.

Results: Here we show that spared nerve injury-induced neuropathic pain alters gut microbial diversity in mice. We successfully constructed reliable microbial interaction networks using the Metagenomic Microbial Interaction Simulator (MetaMIS) and analyzed these networks based on 177,147 simulations. Interestingly, at a higher resolution, our results showed that spared nerve injury-induced neuropathic pain altered both the stability of the microbial community and the key microbes in a gut micro-ecosystem. *Oscillospira*, which was classified as a low-abundance and core microbe, was identified as the key microbe in the Sham group, whereas *Staphylococcus*, classified as a rare and non-core microbe, was identified as the key microbe in the spared nerve injury-induced neuropathic pain group.

Conclusions: In summary, our results provide novel experimental evidence that spared nerve injury-induced neuropathic pain reshapes gut microbial diversity, and alters the stability and key microbes in the gut.

Background

Neuropathic pain is an abnormal perception of pain (Coraggio et al., 2018) that affects 7–10% percent of the human population worldwide (Colloca et al., 2017). Neuropathic pain can cause increased pain sensitivity to mechanical or thermal stimuli (Coraggio et al., 2018). However, current pharmacological treatments for neuropathic pain are still unsatisfactory because the causes of chronic pain cannot always be established (Boccella et al., 2018). One of the current treatments is probiotics (live beneficial microbes), and this is still a growing field. For example, the De Simone Formulation probiotic (i.e., *Bifidobacterium breve*, *B. longum*, *B. infantis*, *Lactobacillus plantarum*, *L. paracasei*, *L. delbrueckii* subsp. *Bulgaricus*, *L. acidophilus*, *Streptococcus thermophilus*) alleviated chemotherapy-induced neuropathic pain in an *in vitro* model, but has not been tested yet *in vivo* (Castelli et al., 2018). A recent study attempted to use probiotics (i.e., *Lactobacillus reuteri* lr06 or *Bifidobacterium* bl5b) to alleviate SNI (spared-nerve injury; a traumatic peripheral nerve injury)-induced neuropathic pain, but failed (Huang et al., 2019).

Host-associated microorganisms have been shown to play important roles in influencing host phenotypes (Costello et al., 2012). For example, gut microbiota can regulate visceral pain sensation in mice (Luczynski et al., 2017). An imbalance of beneficial and harmful host-associated microbes (termed dysbiosis; Manichanh et al., 2012) is associated with Alzheimer's disease (Wang et al., 2019), and could influence host behaviors such as depression and anxiety (Clapp et al., 2017), and also physiological response such as visceral (internal organ) pain (Halfvarson et al., 2017). A recent study showed that the gut microbiota of a host with neuropathic pain after traumatic peripheral nerve injury (spared-nerve injury; SNI) could cause anhedonia (depression-like behavior) to another host through fecal transplantation (Yang et al., 2019). However, the underlying questions around topics such as the interactions and stability of the gut microbiota in a traumatic peripheral nerve injury-induced neuropathic pain model and the key microbes involved (i.e., the microbes that play critical roles) have not been answered.

There are generally two types of network inference methods: similarity-based networks and regression-based networks. Similarity-based networks (or co-occurrence networks) that depend on correlation-based methods are often used to infer ecological interactions, but they are rarely efficient for analyzing these interactions (Hirano and Takemoto, 2019). This is because correlation methods can only infer ecological associations (Hirano and Takemoto, 2019), and cannot interpret more detailed ecological interactions such as the influence of multiple microbial members on a single member, and vice versa (Faust and Raes, 2012). Regression-based networks depend on generalized Lotka–Volterra (gLV) equations to model temporal changes in more than two taxa (Faust and Raes, 2012; Kloppers and Greeff, 2013). The gLV model is one of the most popular models for microbial community ecology studies (Gonze et al., 2018). Microbial interaction networks can be constructed using gLV equations to study the influence of microbial members through positive or negative interactions and determine the stability of the microbial communities. For example, Coyte et al. (2015) constructed microbial interaction networks using gLV equations and suggested that a higher proportion of negative interactions between microbes indicates a stable microbial community maintained by competitive interactions between microbes. In contrast, a higher proportion of positive interactions between microbes indicates an unstable microbial community maintained by cooperative interactions.

Currently, most disease-associated microbiota studies (Catanzaro et al., 2019; Falony et al., 2018; Gentile and Weir, 2018; Lozupone et al., 2012; Zaneveld et al., 2017) have inferred unstable microbial communities or dysbiosis from microbial diversity. This is because microbial diversity may have an inverse association with chronic disease and metabolic dysfunction (Cotillard et al., 2013; Gentile and Weir, 2018). Consequently,

high diversity is generally used to indicate a healthy gut ecosystem (Bäckhed et al., 2012; Falony et al., 2018; Lloyd-Price et al., 2016). However, some scientists argued that there are problems with using diversity to assess health (Brüssow, 2019; Johnson and Burnet, 2016; Shade, 2017). Shade (2017), for example, proposed that high diversity does not necessarily indicate a stable or healthy microbial community. For example, increased microbial diversity in the vagina may have detrimental consequences such as bacterial vaginosis and preterm birth (Brüssow, 2019; Fettweis et al., 2019). In addition, diversity is only an index for the number of taxa in a community and has little ecological value, and a microbial community with high diversity does not necessarily mean that it will remain stable if perturbed (Shade, 2017). Hence, comparing healthy and diseased states using diversity often leads to contradictory results (Johnson and Burnet, 2016). Johnson and Burnet (2016) call for further studies to investigate these using techniques beyond conventional diversity indices and tackle the issue of a lack of analytical methods to assess microbial composition and functioning.

Our objectives were to determine the interactions in and stability of the gut microbiota in a spared nerve injury-induced neuropathic pain model and the key microbes involved**.** The present study used conventional methods (i.e., alpha & beta diversity and differential abundance), but we could not determine the stability of microbial communities or identify the key microbes in mice with SNI or Sham. On the other hand, we successfully constructed reliable microbial interaction networks using Metagenomic Microbial Interaction Simulator (MetaMIS; Shaw et al., 2016) based on gLV equations and analyzed the networks. Interestingly, at a higher resolution, our results showed that neuropathic pain after traumatic peripheral nerve injury alters both the stability of microbial community and the key microbes in a gut micro-ecosystem.

Results

Pain withdrawal threshold decreased after spared nerve injury (SNI)-induced neuropathic pain

We used the SNI model to investigate the influence of traumatic peripheral nerve injury on the interactions and stability of the gut microbiota and its key microbes. To determine the success of surgeries (i.e., SNI and Sham), we evaluated the pain behavior of mice before and after SNI. The behavioral test was conducted 1 day before surgery (-1) as a baseline, and 1, 2, 3, 4, 5, 6, 7, and 14 days after surgery. The timeline of the behavioral test and fecal collection is summarized in Figure 1A. After the traumatic peripheral nerve injury, the paw withdrawal thresholds were significantly lower in the SNI group than in the Sham group on days 1 (p value: 0.033), 2 (p value: 0.003), 4 (p value: 0.020), 5 (p value: 0.003), 6 (p value: 0.049), and 7 (p value: 0.012) (Figure 1B).

Overview of next-generation sequencing metadata

To generate time series data and determine the temporal changes in the gut microbiota, we sequenced 66 purified fecal DNA samples, which were collected over 11 time points (1 day before surgery (-1), and 1, 1.4 (1 day 4 hours), 2, 3, 4, 5, 6, 7, and 14 days after surgery; Figure 1A). In total, we obtained 14,358,275 reads, with an average of 217,550 ± 35,517 reads per sample, and around 16% differences in library size. After we filtered and processed the raw data, we determined the number of OTUs (at the genus level; n=59) from each sample, and illustrated them as rarefaction curves (Supplemental Figure 1). All the rarefaction curves of each time-series sample from the SNI and Sham groups reached an asymptote (Supplemental Figure 1). For the differential relative abundance (based on DESeq2; Benjamini-Hochberg adjusted p-value), 2 genera were found significantly different between groups on days -1-0 (*Roseburia*, p value: 0.001; *Candidate_division_TM7*, p value: 0.01). Four genera (*Roseburia*, p value: 0.000; *Erysipelotrichaceae_Incertae_Sedis*, p value: 0.009; *Mollicutes*_unclassified, p value: 0.012; *Peptococcaceae_unclassified*, p value: 0.013) were found significantly different between groups on days 1-2. Three genera were found significantly different between groups on days 3-5 (*Turicibacter*, p value: 0.000; *Roseburia*, p value: 0.004; *Mollicutes_unclassified*, p value: 0.005). Eight genera were found significantly different between groups on days 6-14 (*Turicibacter*, p value: 0.000; *Allobaculum*, p value: 0.000; *Bifidobacterium*, p value: 0.000; *Akkermansia*, p value: 0.000; *Roseburia*, p value: 0.000; *Mollicutes_unclassified*, p value: 0.009; *Lactobacillus*, p value: 0.013; *Actinobacteria_unclassified*, p value: 0.033). The differential relative abundance of microbes between the SNI and Sham groups is summarized in Supplemental Table 1. To classify the microbial members and track their temporal changes at the genus level, 12 genera were classified as high-abundance and core microbial members: *Bacteroidales_unclassified*, *Bacteroides*, *Desulfovibrio*, *Lachnospiraceae_Incertae_Sedis*, *Lachnospiraceae_unclassified*, *Lactobacillus*, *Moryella*, *Mucispirillum*, *Ruminococcaceae_Insertae_Sedis*, *Ruminococcaceae_unclassified*, *Ruminococcaceae_uncultured*, and *S24-7_unclassified* (Figure 2A/B); 22 genera were classified as low-abundance and core microbial members: *Acetanaerobacterium*, *Adlercreutzia*, *Akkermansia*, *Allobaculum*, *Bacteria_unclassified*, *Candidate_division_TM7*, *Clostridiales_unclassified*, *Clostridium*, *Coriobacteriaceae_unclassified*, *Erysipelotrichaceae_unclassified*, *Firmicutes_unclassified*, *Hydrogenoanaerobacterium*, *Incertae_Sedis*, *Lachnospira*, *Lachnospiraceae_uncultured*, *Oscillibacter*, *Oscillospira*, *Parabacteroides*, *Parasutterella*, *Roseburia*, *Ruminococcus*, and *Turicibacter* (Figure 2C/D); 5 genera were classified as rare and core microbial members: *Barnesiella*, *Eubacterium*, *Family_XIII_Incertae_Sedis*, *Mollicutes_RF9_unclassified*, and *Peptococcaceae_unclassified* (Figure 2E/F); and 20 genera were classified as rare and non-core microbial members: *Acinetobacter*, *Actonobacteria_unclassified*, *Alcaligenes*, *Bacteroidetes_unclassified*, *Bifidobacterium*, *Clostridia_unclassified*, *Clostridium*, *Coprobacillus*, *Enterococcus*, *Escherichia*,

Lactobacillales_unclassified, *Mollicutes_unclassified*, *Olsenella*, *Porphyromonadaceae_unclassified*, *Pseudomonas*, *Robinsoniella*, *Staphylococcus*, *Streptococcus*, and *Weissella* (Figure 2G/H).

Altered gut microbiota diversity and composition

For phylogenetic indices, alpha diversity (at genus level) was evaluated based on non-parametric Shannon's diversity index, inverse Simpson's diversity index, and Chao richness (Figure 3). For non-parametric Shannon's diversity index, the genus diversity of the SNI group on days 6–14 was significantly lower (p value: 0.004) than that of the Sham group on days 6–14. For the inverse Simpson's diversity index, the genus diversity of the SNI group on days 6–14 was significantly lower (p value: 0.040) than that of the Sham group on days 6–14. For both non-parametric Shannon's and inverse Simpson's diversity indexes, the genus diversity of the SNI group on days -1–0 and days 6–14 was not significantly different. For Chao richness, the genus richnesses of the Sham group on days 1–2, 3–5, and 6–14 were significantly lower (p value: 0.006, 0.004, and 0.010, respectively) than those of the Sham group on days -1 to 0. Likewise, the genus richness of the SNI group on days 6–14 was significantly lower (p value: 0.024) than that of the SNI group on days -1 to 0. For beta-diversity (NMDS based on Bray-Curtis dissimilarity), the composition of SNI on day -1 was not significantly different compared to the composition of Sham on day -1, so SNI and Sham on day -1 was grouped together. The composition of SNI and Sham on day -1 was significantly different compared to the composition of SNI on day 6 and the composition of Sham on day 6 (p value: 0.047; Figure 4). The composition of SNI and Sham on days 6 and 14 were all significantly different to each other (p value: 0.048; Figure 4). Interestingly, the composition of SNI on day -1 was not significantly different compared to the composition of SNI on day 14.

Stability of microbial interaction networks

To determine the stability of the microbial communities in the Sham and SNI groups, we constructed complex microbial interaction networks and analyzed the proportion of negative and positive interactions in both groups. In the Sham group, the highest proportion of positive interactions was 9.4E-04 (0.0094) and the lowest proportion of negative interactions was -6.9E-04 (-0.0069; Figure 5). In the Sham group, the highest proportion of positive interactions was 7.5E-04 (0.0075), and the lowest proportion of negative interactions was -9.5E-04 (-0.0095; Figure 5). The proportion of positive interactions in the SNI group was significantly higher than that of the Sham group (p value= 0.008). The proportion of negative interactions in the SNI group was significantly lower than that of the Sham group (p value= 0.044). Also, the bacterial community in the SNI and Sham groups were highly interacting as a whole (no fragmentation), rather than highly interacting in subpopulations (with fragmentation). The complex microbial interaction networks are summarized in Figure 5.

Identification of key microbes

According to the rank that we assigned each genus based on the total rank of betweenness centrality, closeness centrality, and degree centrality, we detected *Oscillospira* and Erysipelotrichaceae_unclassified (rank 1) as the key microbes in the Sham group, followed by *Adlercreutzia* (rank 2) and *Turicibacter* (rank 3) (Supplemental Table 2.1). Oscillospira was identified as the key microbe in the Sham group based on relatively high centrality score (degree: second highest; closeness: fourth highest; betweenness: second highest), with a final rank of 1 (Supplemental Table 2.1). For the SNI group, we detected *Staphylococcus* (rank 1) as the key microbe, followed by *Ruminococcaceae_uncultured* (rank 2) and *Turicibacter* (rank 3) (Supplemental Table 2.2). *Staphylococcus* was identified as the key microbe in the SNI group based on relatively high centrality score (degree: second highest; closeness: thirth highest; betweenness: the highest), with a final rank of 1 (Supplemental Table 2.2). Multiple linear regression showed that the ranks of the betweenness centrality, closeness centrality, and degree centrality were significantly correlated with the final rank of microbes in both the Sham (p value < 0.001; R^2=0.9167) and SNI groups (p value < 0.001; R^2=0.8877; Figure 6).

Interactions between key microbes and other microbes

In the Sham group, *Oscillospira* was influenced by 6 genera through positive interactions and influenced 6 genera through positive interactions. *Oscillospira* was influenced by 5 genera through negative interactions and influenced 13 genera through negative interactions (Table 1 and Supplemental Figure 3A).

In the SNI group, *Staphylococcus* was influenced by 7 genera through positive interactions and influenced 13 genera through positive interactions. *Staphylococcus* was influenced by 7 genera through negative interactions and influenced 3 genera through negative interactions (Table 2 and Supplemental Figure 3B).

Interactions between potential probiotics and other microbes

In the Sham group, potential probiotics such as *Lactobacillus* were influenced by 6 genera through positive interactions and influenced 5 genera through positive interactions. *Lactobacillus* was influenced by 1 genus through negative interactions and influenced 6 genera through negative interactions (Table 3 and Supplemental Figure 3C). Overall, there were two potential probiotics (*Lactobacillus* and *Bifidobacterium*) in this network (Table 3 and Supplemental Figure 3C).

In the Sham group, *Bifidobacterium* was influenced by 2 genera through positive interactions and influenced 2 genera through positive interactions. *Bifidobacterium* was influenced by 7 genera through negative interactions and influenced 1 genus through negative interactions (Table 4 and Supplemental Figure 3E). Overall, there were three potential probiotics (*Bifidobacterium*, *Lactobacillus*, and *Enterococcus*) in this network (Table 4 and Supplemental Figure 3E).

In the SNI group, *Lactobacillus* was influenced by 3 genera through positive interactions and influenced 5 genera through positive interactions. *Lactobacillus* was influenced by 3 genera through negative interactions and did not influence any other microbes through negative interactions (Table 5 and Supplemental Figure 3D). Overall, there was only one potential probiotic (*Lactobacillus*) in this network (Table 5 and Supplemental Figure 3D).

In the SNI group, *Bifidobacterium* was influenced by 1 genus through positive interactions and influenced 7 genera through positive interactions. *Bifidobacterium* was influenced by 5 genera through negative interactions and influenced 1 genus through negative interactions (Table 6 and Supplemental Figure 3F). Overall, there was only one potential probiotic (*Bifidobacterium*) in this network (Table 6 and Supplemental Figure 3F).

Discussion

There is currently a discussion in the academic community about whether microbial diversity can be used to determine the health of a gut environment (Brüssow, 2019; Johnson and Burnet, 2016; Shade, 2017). In our study, we first analyzed microbial diversity to determine the influence of neuropathic pain on the health conditions (i.e., stability) of hosts' gut environments. Even though 2 genera were found significantly different between the SNI and Sham groups on days -1-0 (baselines), which might due to stochastic events, the alpha and beta diversity between groups on days -1-0 were not significantly different. The changes in microbial diversity (i.e., Shannon and Simpson's diversity indices; alpha diversity) in our study were similar to those in a previous study (Yang et al., 2019), in which the microbial diversity in the SNI group was significantly lower than the microbial diversity in the Sham group at the end of the experiment. In contrast, another previous study showed that the microbial diversity between the SNI group with a normal level of vitamin D and the Sham group with a normal level of vitamin D was not significantly different (Guida et al., 2020). Interestingly, the results of the alpha diversity (i.e., the genus diversity of the SNI group on days -1-0 and days 6-14 was not significantly different but the genus diversity of SNI group on days 6-14 was significantly lower than the genus diversity of Sham group on days 6-14) and beta-diversity (i.e., the composition of SNI on day -1 was not significantly different compared to the composition of SNI on day 14) in our study made determining the stability of the microbial community complicated for both groups. To overcome these impediments, we constructed and analyzed complex microbial interaction networks. In accordance with Coyte et al (2015), we found that the Sham group may have a stable gut microbial community due to its high proportion of competitive interactions. In contrast, the SNI group may have an unstable gut microbial community due to its high proportion of cooperative interactions. Even though cooperative interactions may enhance metabolic efficacy, a decrease in the abundance of certain microbes may affect other cooperating microbes, eventually destabilizing the entire microbial community (Coyte et al., 2015). Our results are in accordance with studies (Biggs et al., 2017; Medlock et al., 2018; Venturelli et al., 2018) that suggest that the interactions in the mammalian microbiota are generally competitive and exploitative. For instance, Venturelli et al. (2018) co-cultured a 12-species community and found that 68% of the total interactions were competitive and ammensal, and only 5% were cooperative and commensal. Furthermore, Heinken and Thiele (2015) simulated an 11-species community and found that cooperative and commensal interactions were rare (~10% of total interactions).

Oscillospira, which was classified as a low-abundance and core microbe, was identified as the key microbe (rank 1) in the Sham group, followed by *Adlercreutzia* (rank 2). Previous studies have shown that *Oscillospira* is associated with health (Escobar et al., 2014; Gophna and Konikoff, 2016; Tims et al., 2013; Verdam et al., 2013). For example, *Oscillospira* is enriched in *Christensenella minuta*-altered gut microbial community, which is involved in the promotion of leanness in mice (Goodrich et al., 2014). In a study conducted on human adult monozygotic twins, *Oscillospira* was significantly more abundant in the non-obese twin (lower BMI; Tims et al., 2013); another study, however, found the relative abundance of *Oscillospira* to be significantly lower in obese humans (Verdam et al., 2013). Gophna and Konikoff (2016) suggested that *Oscillospira* is associated with leanness and is probably involved in the promotion of leanness because *Oscillospira* uses host glycans as a food source and causes the host to spend metabolic energy to resynthesize degraded glycoproteins (e.g., gut mucins). Along with its association with leanness, *Oscillospira* can produce butyrate (Gophna et al., 2017), which can protect a host against infections (Leblois et al., 2017) and enhances sleep (Szentirmai et al., 2019).

Like *Oscillospira*, *Adlercreutzia* is also associated with health. According to Euzéby (1997), the genus *Adlercreutzia* contains only one species: *Adlercreutzia equolifaciens*, an equol-producing bacterium (Maruo et al., 2008). Equol is a secondary metabolite of daidzein with a higher anti-carcinogenic activity than daidzein (Liu et al., 2019). Moreover, equol can protect macrophages from oxidative stress caused by microbial lipopolysaccharides, and increase host antioxidants and cytokines (Gou et al., 2015). Liu et al. (2019) showed that the abundance of *Adlercreutzia* decreases in mice with high fat diets. In our study, these beneficial microbes (i.e., *Oscillospira* and *Adlercreutzia*) were the top two key microbes in the Sham group, and this may further support the idea that the microbial interaction network constructed in this study was reliable and the gut ecological environment in the Sham group was stable and healthy.

Along with the interactions among microbes, studies have also shown that the gut microbiota co-evolved with a host to form a mutually beneficial relationship (Ayres, 2013, 2016; Cheng et al., 2019). Hence, the gut microbiota can interact with the host immune system (Fung et al., 2017). For instance, the immune system maintains a stable and healthy gut microbiota by promoting the growth of beneficial gut microbes (Levy et al., 2015; Rooks and Garrett, 2016), whereas a stable and healthy gut microbiota can produce molecular signals that contribute to the development of immune cells and support proper immune responses (Levy et al., 2015; Rooks and Garrett, 2016) to defend against pathogens (Cheng et al., 2019). Hence, along with suffering from chronic pain, the mice with SNI in our study might also have suffered from a weakened immune system due to unstable microbiota communities, probably making them more susceptible to pathogen infection.

Numerous studies showed that the supplementation of probiotics is effective for combating various pathogens (Ayala et al., 2019; Dean et al., 2019; Piewngam et al., 2018) and reducing anxiety and depression-related behavior in mice (Bravo et al., 2011). Huang et al. (2019) attempted to treat neuropathic pain in rats with oral supplementation of probiotics (i.e., *Lactobacillus reuteri* LR06 or *Bifidobacterium* BL5b), but failed. Along with the reasons provided by Huang et al. (2019), we speculate that the treatment failed because key microbes in the rats with neuropathic pain were influenced by and cooperated with the probiotics for survival, and these attenuated the analgesic effects of the probiotics. Interestingly, *Staphylococcus*, the key microbe in the SNI group, influenced *Lactobacillus* through cooperative interactions in our study.

Staphylococcus, which was classified as a rare and non-core microbe, was identified as the key microbe (rank 1) in the SNI group. *Staphylococcus* are infamous for their inflammatory effects on hosts; for example, *Staphylococcus aureus* can cause abscesses, cellulitis, osteomyelitis (Blake et al., 2018; Lowy, 1998), and dermatitis (Nakamura et al., 2013); both *S. aureus* and *S. epidermidis can cause septic arthritis (*Indelli *et al., 2002; Kim and Joo, 2012); and S. saprophyticus can cause pyelonephritis (Chen, 2014; Hur et al., 2016). S. haemolyticus, S. intermedius, S. lugdunensis, S. schleiferi, and S. warneri, however, are infrequent pathogens (Foster, 1996). Other than inflammatory effects, S. aureus can also cause mechanical and thermal hyperalgesia at the hind paw of mice due to pore-forming toxins produced by S. aureus and subsequently cause nociceptor neuron activation (Blake et al., 2018).* Even though *Staphylococcus* was rare in our study, *Staphylococcus* might increase in abundance after two weeks because *Staphylococcus* is an opportunist with fast community succession (*Schulfer et al., 2018*). Rare microbes in certain favorable conditions may occasionally become dominant (Shade et al., 2014) and more important in providing certain functional traits (Chen et al., 2020).

Every method is different and has its own limitations. Some studies removed rare microbial taxa from their analyses—e.g., rare OTUs that might be sequencing artifacts were removed before downstream analyses (Martinson et al., 2017), and rare OTUs were removed from network analyses to reduce false positive results (Weiss et al., 2016). Rarefying data with a big (around 10 times or 1000%) difference in the average sequencing library size can also reduce false positive results (Weiss et al., 2017). However, rarefying data produces false negative results because part of the data is discarded (Weiss et al., 2017). To retain the rare microbial taxa in our study, we did not remove rare OTUs nor did we rarefy our data to equalize sequencing depth. In fact, the differences among average sequencing library sizes in our study were very small (around 16%). Chen et al. (2020) showed that rare microbes might have a more important role in driving multiple functions than do dominant microbes. For instance, rare microbes may influence and change the composition of gut microbiota after a diet change (Benjamino et al., 2018). Rare microbes have also been found to play important roles among host-associated microbes in both animals and plants and enhance host immune systems (Jousset et al., 2017; Stecher et al., 2013; Van der Gast et al., 2011). The current understanding of the ecological role of host-associated rare key microbes in an unstable gut microbial community is still in its infancy and should be investigated further.

Conclusion

In summary, our results provide novel experimental evidence that traumatic peripheral nerve injuries may alter the microbial diversity and stability in the gut, as well as the composition of its key microbes. Nevertheless, the complex microbial interaction networks in our study were simulated based on theoretical analyses. Hence, more biological experiments are required to validate and support our results.

Methods

Animal preparation

All animal procedures conformed to the guidelines specified by the National Institutes of Health and the Institutional Animal Care and Utilization Committee (IACUC), Academia Sinica (Taipei, Taiwan), including the guidelines for the Replacement, Refinement & Reduction of Animals in Research. IACUC approved protocol: 18-12-1246. C57 black 6 (C57BL/6) mice were ordered from the National Laboratory Animal Center (Taipei, Taiwan) and quarantined for a week before any experiment. Six female mice 8 to 12 weeks old were used for the experiment (3 for SNI group, 3 for Sham group). We performed the experiments on female mice because female mice are less aggressive to other female mice than male mice (Tansley et al., 2019). We considered this stress as a confounder in our experiments that might alters the gut microbial diversity and composition. Mice were held under a 12:12-h light-dark cycle with food and water available *ad libitum*. At the end of the experiment, the mice were anesthetized with isoflurane and a mixture of ketamine and xylazine, and sacrificed using cervical dislocation.

Spared-nerve injury model

Surgical procedures were performed under isoflurane anesthesia (liquid inhalation; Aerane, Baxter, USA) according to previous studies (Chang et al., 2019; Shield et al., 2003). After a skin and muscle incision on the left hind limb, the sural nerve and peroneal nerve were tightly ligated using a gamma sterile monofilament with a 3/8 circle taper point (UNIK, Taiwan), then transected. The tibial nerve was not ligated or transected. For the Sham controls, the sural, peroneal, and tibial nerves were exposed but were not ligated or transected. Finally, the skin and muscles were closed using a silk suture.

Behavioral test

A double-blind randomized behavioral test was conducted at room temperature (approximately 25°C) and only during the daytime. Before testing behavior, the mice were habituated on an elevated wire mesh grid for at least 20 min. The mechanical sensitivities of the mice were tested using a Dynamic Plantar Aesthesiometer – DPA (Ugo Basile SRL, Italy), which can automatically detect and record paw-withdrawal thresholds. The stimuli were only applied when the mice were calm with four paws on the mesh grid but not grooming, standing with two hind legs, or sleeping. The behavioral test for mechanical sensitivity was repeated five times for each mouse and the values of pain withdrawal threshold were averaged. The behavioral test was conducted one day before surgery (day -1) as a baseline, and 1, 2, 3, 4, 5, 6, 7, and 14 days after surgery.

Sample collection and DNA extraction

Empty autoclaved containers were aseptically washed with 70% EtOH and sterilized in a laminar flow cabinet with UV light prior to transferring a mouse into each container. In total, 66 fecal samples were collected over two weeks (three mice and 11 time points per group). Fecal samples were collected right after the mice defecated and kept in 2 mL eppendorf tubes in a -80 freezer prior until DNA extraction. The genomic DNA from the fecal samples was extracted using EasyPrep Stool Genomic DNA Kit (TOOLS, Taiwan) and qualified using a Nanodrop spectrophotometer (J&H Technology Co., Ltd, Taiwan).

16S rRNA amplicon preparation and Illumina sequencing

The third and fourth hypervariable regions (V3 and V4) of the small subunit ribosomal RNA gene were amplified using universal eubacterial primers. The forward primer In-341F (5’- TCGTCGGCAGCGTCAGATGTGTATAAGAGACAG-3’) and the reverse primer In-806R (5’-GTCTCGTGGGCTCGGAGATGTGTATAAGAGACAG-3’) were fused with Illumina overhang adapters and sample-specific ten-nucleotide barcodes to allow multiple samples to be analyzed in parallel on a single picotiter plate. The pooled DNA was amplified through PCR (Taq DNA Polymerase 2x Master Mix Red, Biomol, GmbH, Germany), with three replicates, under the following running conditions: initial denaturation at 95°C for 3 min; 24 cycles of 30 s min at 95°C, 30 s at 56°C, 30 s at 72°C; and a final elongation step for 10 min at 72°C. All PCR products were confirmed using 1.5% agarose gel electrophoresis. Three PCR products from each sample were pooled and subsequently isolated from the gel and purified by QIAquick gel extraction kit (Qiagen, Hilden, Germany). The DNA concentration of the cleaned PCR products was determined using a Quant-iT dsDNA HS assay kit and a Qubit fluorometer (Invitrogen, Carlsbad, CA, USA). The amplicons were purified according to the Illumina standard protocol of 16S metagenomic sequencing library preparation, and sequenced on the MiSeq platform with the reagent kit v3. The Illumina fastq files were submitted to the NCBI SRA under accession number PRJNA629058.

Amplicon sequencing data analyses

The Illumina fastq files were de-multiplexed, quality filtered, and analyzed using MOTHUR (Schloss et al., 2009). OTUs (Operational Taxonomic Units) were clustered using UPARSE (Edgar, 2013) with a threshold of 97% pair-wise nucleotide sequence identity, and the cluster centroid for each OTU was chosen as the OTU representative sequence. OTU representative sequences were classified taxonomically using MOTHUR based on the SILVA reference database, with k-nearest neighbor consensus and Wang method, using 80% confidence as the threshold for taxonomic assignment. OTUs were determined to the genus level for these analyses. OTUs clustered at 97% that could not be assigned to a genus were assigned to a family, order, or class, and were included in the analyses. The microbial members were classified as: high-abundance (average sequencing reads more than 1% of the total sequencing reads across all time-series samples), low-abundance (average sequencing reads ranged from 0.1% to 1%), rare (average sequencing reads lower than 0.1%), core (present in all time-series samples), or non-core (present only in certain time-series samples). For alpha diversity, non-parametric Shannon's diversity index, Inverse Simpson's diversity index, and Chao richness were calculated using MOTHUR (Schloss et al., 2009). To increase the statistical power for the analysis of alpha diversity, we combined the time points into the following: days -1 to 0 (6 samples), days 1–2 (6), days 3–5 (9), and days 6–14 (9). The beta diversity was illustrated using 2-dimensional non-metric multidimensional scaling (NMDS) plots of 3-dimensional data and calculated in R (vegan package; Oksanen et al., 2019). Both alpha and beta diversities were performed at the genus level.

Parameters for inferring reliable microbial interaction networks

In MetaMIS, using generalized Lotka Volterra equations, each microbial interaction network was inferred based on 177,147 (3^{11}; three fecal samples and 11 time points per group) simulations. Positive or negative interactions between two nodes (i.e., OTUs at the genus level) with a permutation cutoff >70% (124003/177147) were considered reliable positive or negative interactions.

Topological inferences from the microbial interaction network

Gephi was used, with each node representing an OTU (at the genus level) and each edge representing the interaction between two OTUs. The key OTUs that may play important roles in an interaction network were determined based on betweenness centrality, closeness centrality, and degree, and were positioned at the center of the network. Degree centrality measures the number of edges connecting an OTU with other OTU in the network (Layeghifard et al., 2017). As the number of edges connecting an OTU with other OTU increases, the degree centrality of the OTU increases. Degree is indicated by node color; a redder node corresponds to a higher value of degree. Betweenness centrality measures the number of times an OTU serves as a bridge along the shortest path between two other OTU. As the frequency of an OTU serves as a bridge increases, the betweenness centrality of the OTU increases (Ai et al., 2019). Betweenness centrality is indicated by node size; a larger node corresponds to a higher value of betweenness centrality. Closeness centrality measures the sum of the length of the shortest path between an OTU and other OTU in the network (Layeghifard et al., 2017). As the closeness centrality of an OTU increases, the OTU will be positioned closer to the center of the network, thus closer to other OTU (Ai et al., 2019). Closeness centrality is indicated by text size; larger text corresponds to a higher value of closeness centrality. The strength of the interaction between two nodes is indicated by color; the redder the edge, the more positive the interaction between its two corresponding nodes, and the bluer the edge, the more negative the interaction between its two nodes.

A rank was assigned to each OTU in the SNI and Sham groups based on the centrality score (degree, closeness and betweenness). For example, the higher the degree centrality score of an OTU, the higher the rank of the OTU based on degree centrality. Total rank is the sum of rank based on degree, closeness and betweenness centrality. A final rank was assigned to each OTU based on the total rank. The OTU with the highest final rank will be the key microbe.

Statistical analyses

DESeq2 was used to analyze the differential relative abundance of microbes between the SNI and Sham groups (based on Benjamini-Hochberg adjusted p-value; Love et al., 2014). A permutation two sample t-test was used to analyze alpha-diversity. For beta-diversity, PERMANOVA (permutational multivariate analysis of variance) was used to analyze the microbiome data. The Shapiro–Wilk test was used to determine the normality of the proportion of positive and negative interactions in the SNI and Sham groups. The dataset of the relative positive and negative interactions in the SNI and Sham groups was not normally distributed. Hence, a Wilcoxon rank sum test was used to determine the difference in the proportions of positive or negative interactions between the SNI and Sham groups. To confirm the final rank assigned to each OTU, multiple linear regression analyses were conducted to examine the correlation between the final rank of OTU and the rank of centrality (degree, closeness, and betweeness). Statistical analyses were conducted using R (R Development Core Team, 2008). p values < 0.05 were considered significant.

Abbreviations

gLV: Generalized Lotka–Volterra

IACUC: Institutional Animal Care and Utilization Committee

MetaMIS: Metagenomic Microbial Interaction Simulator

OTU: Operational taxonomic unit

PCR: Polymerase chain reaction
PERMANOVA: permutational multivariate analysis of variance

rRNA: Ribosomal ribonucleic acid

SNI: Spared-Nerve Injury

SRA: Sequence Read Archive

Declarations

Ethics approval and consent to participate

All animal procedures conformed to the National Institutes of Health guidelines in accordance with the guidelines specified by the Institutional Animal Care and Utilization Committee (IACUC), Academia Sinica (Taipei, Taiwan). IACUC approval protocol: 18-12-1246.

Consent for publication

Not applicable

Availability of data and materials

The Illumina fastq files are available in the NCBI SRA under accession number PRJNA629058. The other datasets used and/or analyzed during the current study are available from the corresponding author upon reasonable request.

Competing interests

The authors declare that they have no competing interests.

Funding

This work was financially supported by the MOST 108-2311-B-001-031. The funder had no role in the study design, data collection, and interpretation, or the decision to submit the work for publication.

Authors' contributions

GJBM conducted the experiment, analyzed and interpreted the data, and drafted the manuscript. GTWS conducted 177,147 interaction network simulations. WHC contributed to the guidance of the animal behavior test and surgeries. DW and CCC helped guide the study and supervise the research. All authors read, contributed to, and approved the final manuscript.

Acknowledgements

We thank Le Hanh and Cheng-Yu Chen for their assistance troubleshooting the MOTHUR-UPARSE pipeline. Thanks also to Noah Last of Third Draft Editing for editing the manuscript's English.

References

Ai D, Pan H, Li X, Wu M, Xia LC. Association network analysis identifies enzymatic components of gut microbiota that significantly differ between colorectal cancer patients and healthy controls. PeerJ. 2019; 7:e7315.

Ayres JS. Cooperative microbial tolerance behaviors in host-microbiota mutualism. Cell. 2016; 165:1323-1331.

Ayres JS. Inflammasome-microbiota interplay in host physiologies. Cell Host Microbe. 2013; 14:491-497.

Ayala DI, Cook PW, Franco JG, Bugarel M, Kottapalli KR, Loneragan GH, et al. A systematic approach to identify and characterize the effectiveness and safety of novel probiotic strains to control foodborne pathogens. Front Microbiol. 2019; 10:1108.

Bäckhed F, Fraser CM, Ringel Y, Sanders ME, Sartor RB, Sherman PM, et al. Defining a healthy human gut microbiome: current concepts, future directions, and clinical applications. Cell Host Microbe. 2012; 12:611-622.

Benjamino J, Lincoln S, Srivastava R, Graf J. Low-abundant bacteria drive compositional changes in the gut microbiota after dietary alteration. Microbiome. 2018; 6:86.

Biggs MB, Medlock GL, Moutinho TJ, Lees HJ, Swann JR, Kolling GL, Papin JA. Systems-level metabolism of the altered Schaedler flora, a complete gut microbiota. ISME. 2017; 11, 426-438.

Blake KJ, Baral P, Voisin T, Lubkin A, Pinho-Ribeiro FA, Adams KL, et al. Staphylococcus aureus produces pain through pore-forming toxins and neuronal TRPV1 that is silenced by QX-314. Nat Commun. 2018; 9:37.

Boccella S, Guida F, Palazzo E, Marabese I, de Novellis V, Maione S, Luongo L. Spared nerve injury as a long-lasting model of neuropathic pain. Methods Mol Biol. 2018; 1727:373-378.

Bravo JA, Forsythe P, Chew MV, Escaravage E, Savignac HM, Dinan TG, et al. Ingestion of Lactobacillus strain regulates emotional behavior and central GABA receptor expression in a mouse via the vagus nerve. Proc Natl Acad Sci U S A. 2011; 108:16050-1655.

Brüssow H. Problems with the concept of gut microbiota dysbiosis. Microb Biotechnol. 2019; 13:423-434.

Castelli V, Palumbo P, d'Angelo M, Moorthy NK, Antonosante A, Catanesi M, et al. Probiotic DSF counteracts chemotherapy induced neuropathic pain. Oncotarget. 2018; 9:27998-28008.

Catanzaro JR, Strauss JD, Bielecka A, Porto AF, Lobo FM, Urban A. IgA-deficient humans exhibit gut microbiota dysbiosis despite secretion of compensatory IgM. Sci Rep. 2019; 9:13574.

Chang YT, Chen WH, Shih HC, Min MY, Shyu BC, Chen CC. Pain. 2019; 160:1208-1223. Chen CH. Staphylococcus saprophyticus bacteremia with pyelonephritis cured by gentamicin. J Formos Med Assoc. 2014; 113:483-484.

Chen QL, Ding J, Zhu D, Hu HW, Delgado-Baquerizo M, Ma YB, et al. Rare microbial taxa as the major drivers of ecosystem multifunctionality in long-term fertilized soils. Soil Biol Biochem. 2020; 141:107686.

Chen WH, Chang YT, Chen YC, Cheng SJ, Chen CC. Spinal PKC/ERK signal pathway mediates hyperalgesia priming. Pain. 2018; 159:907-918.

Cheng HY, Ning MX, Chen DK, Ma WT. Interactions between the gut microbiota and the host innate immune response against pathogens. Front Immunol. 2019; 10:607.

Clapp M, Aurora N, Herrera L, Bhatia M, Wilen E, Wakefield S: Gut microbiota's effect on mental health: The gut-brain axis. Clin Pract. 2017; 7:987.

Colloca L, Ludman T, Bouhassira D, Baron R, Dickenson AH, Yarnitsky D, et al. Neuropathic pain. Nat Rev Dis Primers. 2017; 3:17002.

Coraggio V, Guida F, Boccella S, Scafuro M, Paino S, Romano D, et al. Neuroimmune-driven neuropathic pain establishment: A focus on gender differences. Int J Mol Sci. 2018; 19:pii:E281.

Cotillard A, Kennedy SP, Kong LC, Prifti E, Pons N, Le Chatelier E, et al. Dietary intervention impact on gut microbial gene richness. Nature. 2013; 500:585-588.

Coyte KZ, Schluter J, Foster KR. The ecology of the microbiome: Networks, competition, and stability. Science. 2015; 350:663-666.

Dean SN, Leary DH, Sullivan CJ, Oh E, Walper SA. Isolation and characterization of Lactobacillus-derived membrane vesicles. Sci Rep. 2019; 9:877.

Edgar RC. UPARSE: highly accurate OTU sequences from microbial amplicon reads. Nat Methods. 2013; 10:996-998.

Escobar JS, Klotz B, Valdes BE, Agudelo GM. The gut microbiota of Colombians differs from that of Americans, Europeans and Asians. BMC Microbiol. 2014; 14:311.

Euzéby JP. List of bacterial names with standing in nomenclature: a folder available on the Internet. Int J Syst Bacteriol. 1997; 47:590-592.

Falony G, Vieira-Silva S, Raes J. Richness and ecosystem development across faecal snapshots of the gut microbiota. Nat Microbiol. 2018; 3:526-528.

Faust K, Raes J. Microbial interactions: from networks to models. Nat Rev Microbiol. 2012 Jul;10:538-550.

Fettweis JM, Serrano MG, Brooks JP, Edwards DJ, Girerd PH, Parikh HI, et al. The vaginal microbiome and preterm birth. Nat Med. 2019; 25:1012-1021.

Foster T. Staphylococcus. In: Baron S, editor. Medical Microbiology. 4th edition. Galveston (TX): University of Texas Medical Branch at Galveston; 1996. Chapter 12. Available from: https://www.ncbi.nlm.nih.gov/books/NBK8448/

Fung TC, Olson CA, Hsiao EY. Interactions between the microbiota, immune and nervous systems in health and disease. Nat Neurosci. 2017; 20:145-155.

Gentile CL, Weir TL. The gut microbiota at the intersection of diet and human health. Science. 2018; 362:776-780.

Gonze D, Coyte KZ, Lahti L, Faust K. Microbial communities as dynamical systems. Curr Opin Microbiol. 2018; 44:41-49.

Goodrich JK, Waters JL, Poole AC, Sutter JL, Koren O, Blekhman R, et al. Human genetics shape the gut microbiome. Cell. 2014; 159:789-799.

Gophna U, Konikoff T, Nielsen HB. Oscillospira and related bacteria - From metagenomic species to metabolic features. Environ Microbiol. 2017; 19:835-841.

Gou Z, Jiang S, Zheng C, Tian Z, Lin X. Equol inhibits LPS-induced oxidative stress and enhances the immune response in chicken HD11 macrophages. Cell Physiol Biochem. 2015; 36:611-621.

Guida F, Boccella S, Belardo C, Iannotta M, Piscitelli F, De Filippis F, et al. Altered gut microbiota and endocannabinoid system tone in vitamin D deficiency-mediated chronic pain. Brain Behav Immun. 2020; 85:128-141.

Halfvarson J, Brislawn CJ, Lamendella R, Vázquez-Baeza Y, Walters WA, Bramer LM, et al. Dynamics of the human gut microbiome in inflammatory bowel disease. Nat Microbiol. 2017; 2:17004.

Heinken A, Thiele I. Anoxic conditions promote species-specific mutualism between gut microbes in silico. Appl Environ Microbiol. 2015; 81:4049-4061.

Hirano H, Takemoto K. Difficulty in inferring microbial community structure based on co-occurrence network approaches. BMC Bioinformatics. 2019; 20:329.

Huang J, Zhang C, Wang J, Guo Q, Zou W. Oral Lactobacillus reuteri LR06 or Bifidobacterium BL5b supplement do not produce analgesic effects on neuropathic and inflammatory pain in rats. Brain Behav. 2019;9:e01260.

Hur J, Lee A, Hong J, Jo WY, Cho OH, Kim S, Bae IG. Staphylococcus saprophyticus bacteremia originating from urinary tract infections: A Case Report and Literature Review. Infect Chemother. 2016; 48:136-139.

Indelli PF, Dillingham M, Fanton G, Schurman DJ. Septic arthritis in postoperative anterior cruciate ligament reconstruction. Clin Orthop Relat Res. 2002; 398:182-188.

Johnson KV, Burnet PW. Microbiome: Should we diversify from diversity? Gut Microbes. 2016; 7:455-458.

Jousset A, Bienhold C, Chatzinotas A, Gallien L, Gobet A, Kurm V, et al. Where less may be more: how the rare biosphere pulls ecosystems strings. ISME J. 2017; 11:853-862.

Kim YM, Joo YB. Clinical presentation of Staphylococcus epidermidis septic arthritis following anterior cruciate ligament reconstruction. Knee Surg Relat Res. 2012; 24:46-51.

Kloppers PH, Greeff JC. Lotka–Volterra model parameter estimation using experiential data. Appl Math Comput. 2013; 224:817–825.

Layeghifard M, Hwang DM, Guttman DS. Disentangling Interactions in the Microbiome: A Network Perspective. Trends Microbiol. 2017; 25:217-228.

Leblois J, Massart S, Li B, Wavreille J, Bindelle J, Everaert N. Modulation of piglets' microbiota: differential effects by a high wheat bran maternal diet during gestation and lactation. Sci Rep. 2017; 7:7426.

Levy M, Thaiss CA, Elinav E. Metagenomic cross-talk: the regulatory interplay between immunogenomics and the microbiome. Genome Med. 2015; 7:120.

Liu Y, Wu X, Jiang H. High dietary fat intake lowers serum equol concentration and promotes prostate carcinogenesis in a transgenic mouse prostate model. Nutr Metab (Lond). 2019; 16:24.

Lloyd-Price J, Abu-Ali G, Huttenhower C. The healthy human microbiome. Genome Med. 2016; 8:51.

Love MI, Huber W, Anders S. Moderated estimation of fold change and dispersion for RNA-seq data with DESeq2. Genome Biol. 2014; 15:550.

Lowy FD. Staphylococcus aureus infections. N. Engl. J. Med. 1998; 339:520-532.

Lozupone CA, Stombaugh J, Gordon J, Jansson JK, Knight R. Diversity, stability and resilience of the human gut microbiota. Nature. 2012; 489:220-230.

Luczynski P, Tramullas M, Viola M, Shanahan F, Clarke G, O'Mahony S, et al. Microbiota regulates visceral pain in the mouse. Elife. 2017; 6:e25887.

Manichanh C, Borruel N, Casellas F, Guarner F. The gut microbiota in IBD. Nat Rev Gastroenterol Hepatol. 2012; 9:599-608.

Martinson VG, Douglas AE, Jaenike J. Community structure of the gut microbiota in sympatric species of wild drosophila. Ecol Lett. 2017; 20:629-639.

Maruo T, Sakamoto M, Ito C, Toda T, Benno Y. Adlercreutzia equolifaciens gen. nov., sp. nov., an equol-producing bacterium isolated from human faeces, and emended description of the genus Eggerthella. Int. J. Syst. Evol. Microbiol. 2008; 58:1221-1227.

Medlock GL, Carey MA, McDuffie DG, Mundy MB, Giallourou N, Swann JR, et al. Inferring metabolic mechanisms of interaction within a defined gut microbiota. Cell Syst. 2018; 7: 245-257.

Nakamura Y, Oscherwitz J, Cease KB, Chan SM, Muñoz-Planillo R, Hasegawa M, et al. Staphylococcus δ-toxin induces allergic skin disease by activating mast cells. Nature. 2013; 503:397-401.

Oksanen J, Blanchet FG, Friendly M, Kindt R, Legendre P, McGlinn D, et al. vegan: Community Ecology Package. R package version 2.5-6. 2019. https://CRAN.R-project.org/package=vegan

Piewngam P, Zheng Y, Nguyen TH, Dickey SW, Joo HS, Villaruz AE, et al. Pathogen elimination by probiotic Bacillus via signalling interference. Nature. 2018; 562:532-537.

Rooks MG, Garrett WS. Gut microbiota, metabolites and host immunity. Nat Rev Immunol. 2016; 16:341-352.

Schloss PD, Westcott SL, Ryabin T, Hall JR, Hartmann M, Hollister EB, et al. Introducing mothur: open-source, platform-independent, community-supported software for describing and comparing microbial communities. Appl Environ Microbiol. 2009; 75:7537-7541.

*Schulfer AF, Battaglia T, Alvarez Y, Bijnens L, Ruiz VE, Ho M, et al. Intergenerational transfer of antibiotic-perturbed microbiota enhances colitis in susceptible mice. Nat Microbiol. 2018; 3:234-242.*Shade, A. Diversity is the question, not the answer. ISME J. 2017; 11:1-6.

Shade A. Diversity is the question, not the answer. ISME J. 2017; 11:1-6.

Shade A, Jones SE, Caporaso JG, Handelsman J, Knight R, Fierer N, Gilbert JA. Conditionally rare taxa disproportionately contribute to temporal changes in microbial diversity. mBio. 2014; 5:e01371-14.

Shaw GT, Pao YY, Wang D. MetaMIS: a metagenomic microbial interaction simulator based on microbial community profiles. BMC Bioinformatics. 2016; 17:488.

Shields SD, Eckert WA 3rd, Basbaum AI. Spared nerve injury model of neuropathic pain in the mouse: a behavioral and anatomic analysis. J Pain. 2003; 4:465-470.

Stecher B, Berry D, Loy A. Colonization resistance and microbial ecophysiology: using gnotobiotic mouse models and single-cell technology to explore the intestinal jungle. FEMS Microbiol Rev. 2013; 37:793-829.

Stein RR, Bucci V, Toussaint NC, Buffie CG, Rätsch G, Pamer EG, et al. Ecological modeling from time-series inference: insight into dynamics and stability of intestinal microbiota. PLoS Comput Biol. 2013; 9:e1003388.

Szentirmai É, Millican NS, Massie AR, Kapás L. Butyrate, a metabolite of intestinal bacteria, enhances sleep. Sci Rep. 2019; 9:7035.

Tansley SN, Tuttle AH, Wu N, Tohyama S, Dossett K, Gerstein L, et al. Modulation of social behavior and dominance status by chronic pain in mice. Genes Brain Behav. 2019; 18:e12514.

Tims S, Derom C, Jonkers DM, Vlietinck R, Saris WH, Kleerebezem M, et al. Microbiota conservation and BMI signatures in adult monozygotic twins. ISME J. 2013; 7:707-717.

Van der Gast CJ, Walker AW, Stressmann FA, Rogers GB, Scott P, Daniels TW, Carroll MP, et al. Partitioning core and satellite taxa from within cystic fibrosis lung bacterial communities. ISME J. 2011; 5:780-791.

Venturelli OS, Carr AC, Fisher G, Hsu RH, Lau R, Bowen BP, et al. Deciphering microbial interactions in synthetic human gut microbiome communities. Mol. Syst. Biol. 2018; 14:e8157.

Verdam FJ, Fuentes S, de Jonge C, Zoetendal EG, Erbil R, Greve JW, Buurman WA, de Vos WM, Rensen SS. Human intestinal microbiota composition is associated with local and systemic inflammation in obesity. Obesity (Silver Spring). 2013; 21:E607-E615.

Wang X, Sun G, Feng T, Zhang J, Huang X, Wang T, et al. Sodium oligomannate therapeutically remodels gut microbiota and suppresses gut bacterial amino acids-shaped neuroinflammation to inhibit Alzheimer's disease progression. Cell Res. 2019;29:787-803.

Weiss S, Van Treuren W, Lozupone C, Faust K, Friedman J, Deng Y, et al. Correlation detection strategies in microbial data sets vary widely in sensitivity and precision. ISME J. 2016; 10:1669-1681.

Weiss S, Xu ZZ, Peddada S, Amir A, Bittinger K, Gonzalez A, et al. Normalization and microbial differential abundance strategies depend upon data characteristics. Microbiome. 2017; 5:27.

Yang C, Fang X, Zhan G, Huang N, Li S1, Bi J, et al., Key role of gut microbiota in anhedonia-like phenotype in rodents with neuropathic pain. Transl Psychiatry. 2019; 9:57.

Zaneveld JR, McMinds R, Vega Thurber R. Stress and stability: applying the Anna Karenina principle to animal microbiomes. Nat Microbiol. 2017; 2:17121.

Tables

Table 1. Interactions between *Oscillospira* and other microbes in the Sham group.

Oscillospira was influenced by other microbes through positive (+) interactions	*Oscillospira* was influenced by other microbes through negative (-) interactions	*Oscillospira* influenced other microbes through positive (+) interactions	*Oscillospira* influenced other microbes through negative (-) interactions
Barnesiella	*Clostridiales_unclassified*	*Acetanaerobacterium*	*Actinobacteria_unclassified*
Erysipelotrichaceae_unclassified	*Firmicutes_unclassified*	*Bacteroidales_unclassified*	*Akkermansia*
Lactobacillus	*Peptococcaceae*	*Clostridium_Candidatus_Arthromitus*	*Allobaculum*
Mollicutes_RF9	*Ruminococcus*	*Lachnospiraceae_unclassified*	*Bacteroidales_S24-7*
Mollicutes_unclassified	*Ruminococcaceae_unclassified*	*Porphyromonadaceae_unclassified*	*Bifidobacterium*
Streptococcus		*Ruminococcaceae_Incertae_Sedis*	*Clostridium_unclassified*
			Olsenella
			Parabacteroides
			Parasutterella
			Peptococcaceae_unclassified
			Ruminococcaceae_uncultured
			Ruminococcus
			Turicibacter

Table 2. Interactions between *Staphylococcus* and other microbes in the SNI group.

Staphylococcus was influenced by other microbes through positive (+) interactions	*Staphylococcus* was influenced by other microbes through negative (-) interactions	*Staphylococcus* influenced other microbes through positive (+) interactions	*Staphylococcus* influenced other microbes through negative (-) interactions
Bacteroides	*Bacteroidales_unclassified*	*Bacteria_unclassified*	*Akkermansia*
Clostridium_unclassified	*Candidate_division_TM7*	*Clostridiales_unclassified*	*Bacteroidales_S24-7*
Erysipelotrichaceae_Incertae_Sedis	*Eubacterium*	*Desulfovibrio*	*Lactobacillus*
Lachnospira	*Lachnospiraceae_unclassified*	*Firmicutes_unclassified*	
Parabacteroides	*Mollicutes_unclassified*	*Hydrogenoanaerobacterium*	
Ruminococcus	*Roseburia*	*Lachnospiraceae_Incertae_Sedis*	
Turicibacter	*Ruminococcaceae_Incertae_Sedis*	*Lachnospiraceae_unclassified*	
		Lachnospiraceae_uncultured	
		Mucispirillum	
		Oscillibacter	
		Oscillospira	
		Ruminococcaceae_Incertae_Sedis	
		Ruminococcaceae_unclassified	

Table 3. Interactions between *Lactobacillus* and other microbes in the Sham group.

Lactobacillus was influenced by other microbes through positive (+) interactions	*Lactobacillus* was influenced by other microbes through negative (-) interactions	*Lactobacillus* influenced other microbes through positive (+) interactions	*Lactobacillus* influenced other microbes through negative (-) interactions
Clostridium_unclassified	*Clostridia_unclassified*	*Desulfovibrio*	*Adlercreutzia*
Eubacterium		*Lachnospiraceae_uncultured*	*Bifidobacterium*
Firmicutes_unclassified		*Oscillibacter*	*Coprobacillus*
Parabacteroides		*Ruminococcaceae_Incertae_Sedis*	*Porphyromonadaceae_unclassified*
Parasutterella		*Ruminococcaceae_unclassified*	*Ruminococcus*
Ruminococcus			*Turicibacter*

Table 4. Interactions between *Bifidobacterium* and other microbes in the Sham group.

Bifidobacterium was influenced by other microbes through positive (+) interactions	*Bifidobacterium* was influenced by other microbes through negative (-) interactions	*Bifidobacterium* influenced other microbes through positive (+) interactions	*Bifidobacterium* influenced other microbes through negative (-) interactions
Adlercreutzia	*Lactobacillus*	*Acinetobacter*	*Coriobacteriaceae_unclassified*
Turicibacter	*Bacteroidales_S24-7*	*Ruminococcus*	
	Erysipelotrichaceae_unclassified		
	Barnesiella		
	Enterococcus		
	Mollicutes_unclassified		
	Oscillospira		

Table 5. Interactions between *Lactobacillus* and other microbes in the SNI group.

Lactobacillus was influenced by other microbes through positive (+) interactions	*Lactobacillus* was influenced by other microbes through negative (-) interactions	*Lactobacillus* influenced other microbes through positive (+) interactions	*Lactobacillus* influenced other microbes through negative (-) interactions
Hydrogenoanaerobacterium	*Bacteroidales_unclassified*	*Bacteria_unclassified*	None
Parasutterella	*Barnesiella*	*Clostridiales_unclassified*	
Staphylococcus	*Lachnospiraceae_unclassified*	*Desulfovibrio*	
		Lachnospiraceae_uncultured	
		Parabacteroides	

Table 6. Interactions between *Bifidobacterium* and other microbes in the SNI group.

Bifidobacterium was influenced by other microbes through positive (+) interactions	*Bifidobacterium* was influenced by other microbes through negative (-) interactions	*Bifidobacterium* influenced other microbes through positive (+) interactions	*Bifidobacterium* influenced other microbes through negative (-) interactions
Acetanaerobacterium	*Akkermansia*	*Acetanaerobacterium*	*Allobaculum*
	Clostridium_Candidatus_Arthromitus	*Barnesiella*	
	Lachnospiraceae_uncultured	*Candidate_division_TM7*	
	Ruminococcus	*Erysipelotrichaceae_unclassified*	
	Turicibacter	*Eubacterium*	
		Mollicutes_RF9	
		Ruminococcaceae_uncultured	

Figures

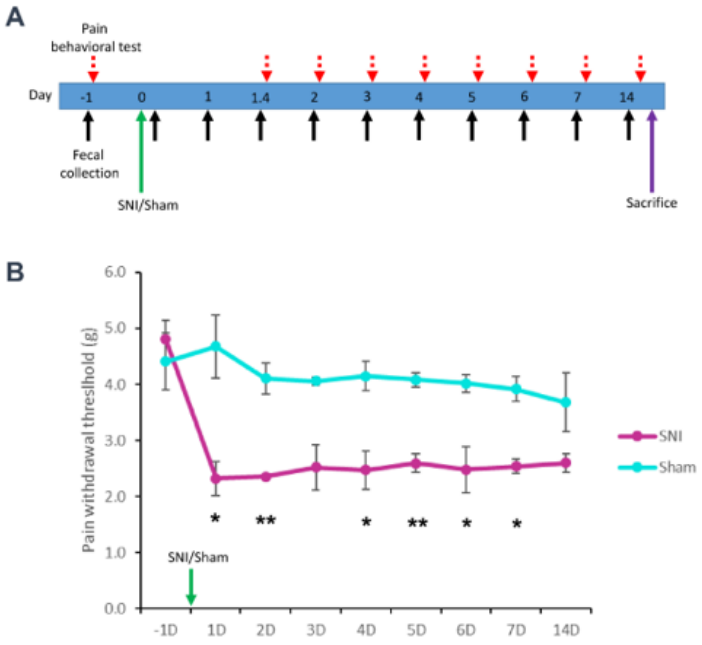

Figure 1

The timeline for fecal collection and pain behavioral test. A) Day -1 is the baseline. The SNI and Sham groups were tested on day 0. B) Student's T test (* p< 0.05, **p< 0.01, SNI group VS Sham group; sample size (n)=6). Data are shown as mean ± S.E.M.

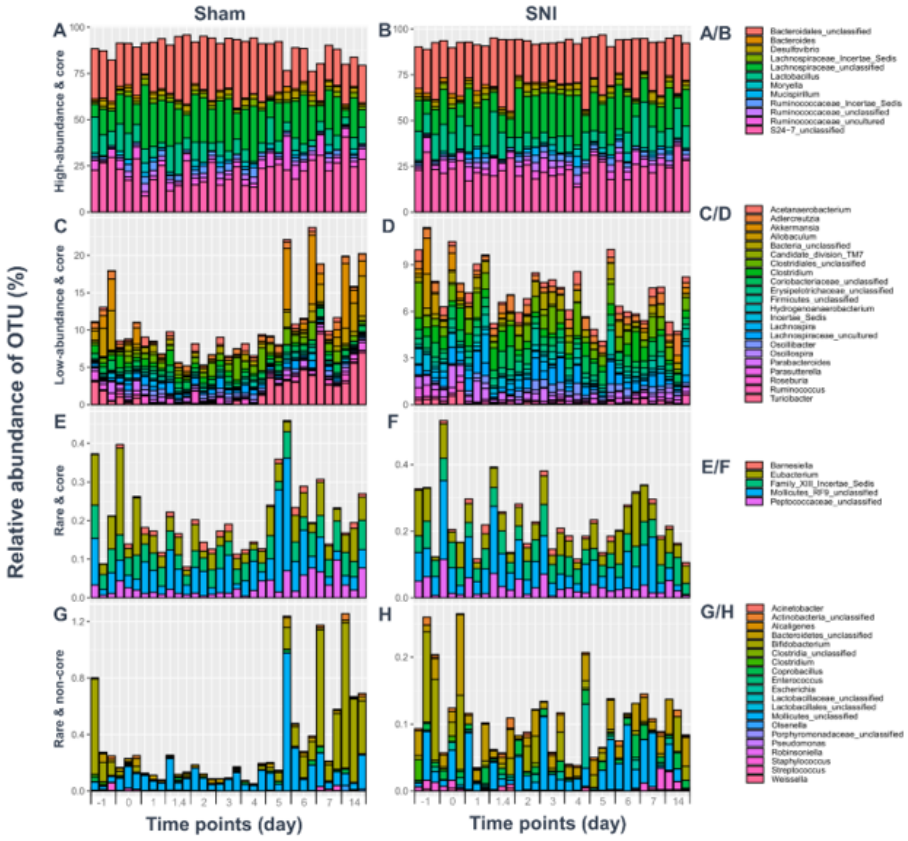

Figure 2

The classification and temporal change of microbial members at the genus level. Microbial members were partitioned based on: (A/B) high-abundance & core; (C/D) low-abundance & core; (E/F) rare & core; (G/H) rare & non-core.

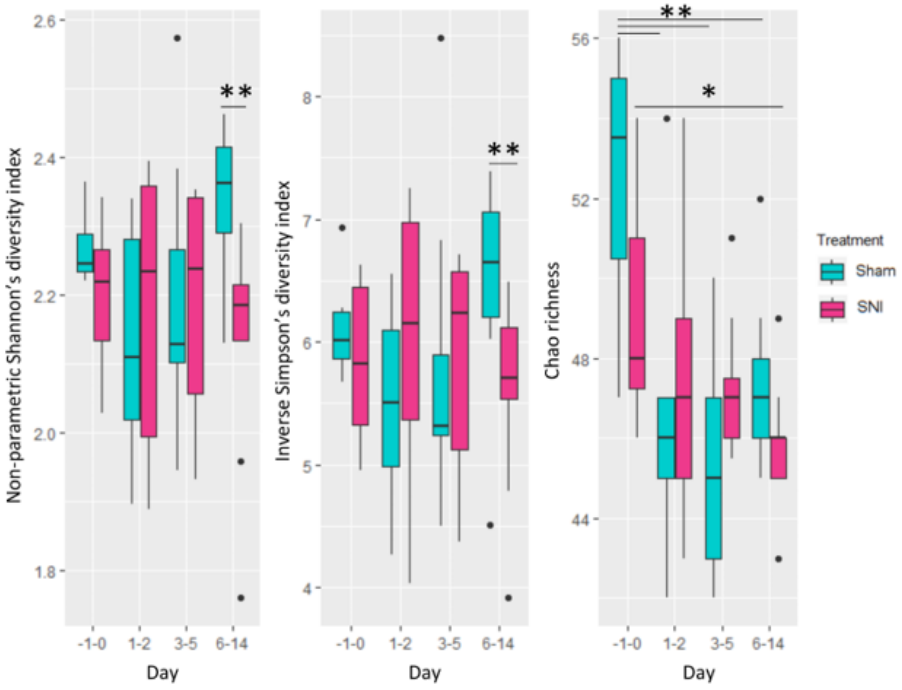

Figure 3

Boxplots of alpha diversity based on non-parametric Shannon's diversity index, inverse Simpson's diversity index, and Chao richness. Permutation two sample t-test (* p< 0.05, ** p< 0.01). Days -1–0: n=6; Days 1–2: n=6; Days 3–5: n=9; Days 6–14: n=9.

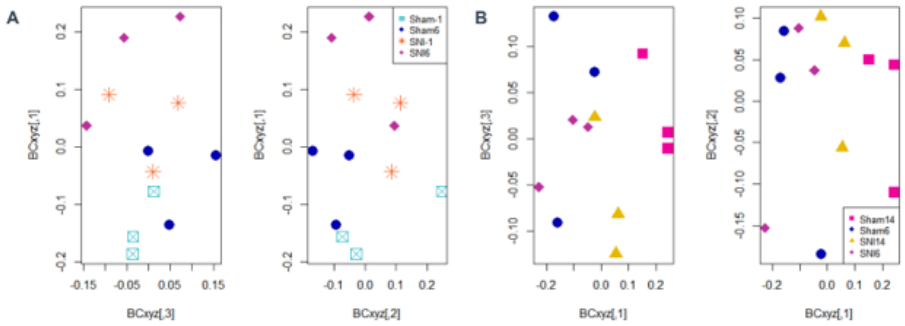

Figure 4

2D plots of 3D NMDS data based on Bray-Curtis dissimilarity. A) SNI and Sham on day -1 are not significantly different (PERMANOVA: p value = 0.7), thus combined as a group and showed significantly different with SNI and Sham groups on day 6 (PERMANOVA: p value = 0.047; n=12); B) All SNI and Sham groups on days 6 and 14 are significantly different (PERMANOVA: p value = 0.048; n=12).

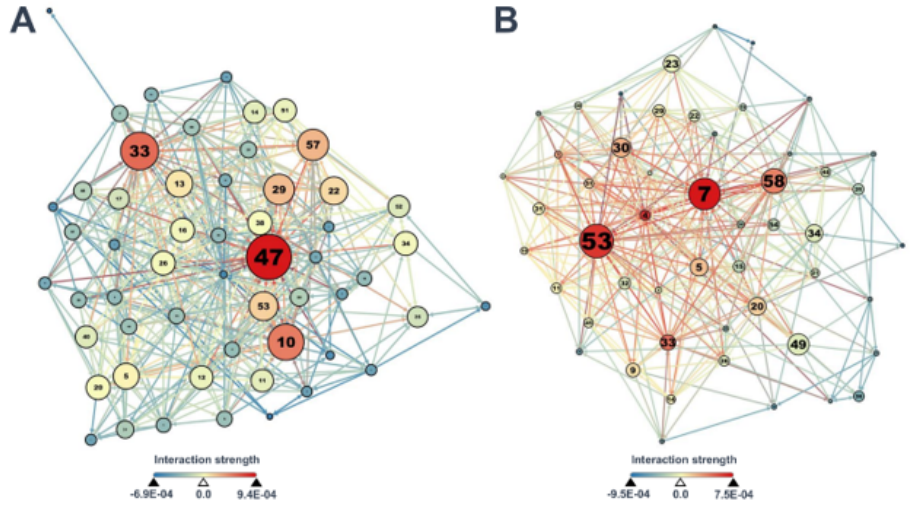

OTU	Taxonomy
Otu01	*Lachnospiraceae_unclassified*
Otu02	*Bacteroidales_S24-7*
Otu03	*Bacteria_unclassified*
Otu04	*Bacteroidales_unclassified*
Otu05	*Ruminococcaceae_unclassified*
Otu06	*Clostridiales_unclassified*
Otu07	*Ruminococcaceae_uncultured*
Otu08	*Lachnospiraceae_Incertae_Sedis*
Otu09	*Firmicutes_unclassified*
Otu10	*Ruminococcaceae_Incertae_Sedis*
Otu11	*Lachnospiraceae_uncultured*
Otu12	*Mollicutes_RF9*
Otu13	*Adlercreutzia*
Otu14	*Bacteroidetes_unclassified*
Otu15	*Erysipelotrichaceae_unclassified*
Otu16	*Coriobacteriaceae_unclassified*
Otu17	*Lactobacillus*
Otu18	*Moryella*
Otu19	*Clostridiales_Family_XIII_Incertae_Sedis*
Otu20	*Oscillibacter*

OTU	Taxonomy
Otu21	*Acetanaerobacterium*
Otu22	*Bacteroides*
Otu23	*Barnesiella*
Otu24	*Coprobacillus*
Otu25	*Allobaculum*
Otu26	*Oscillospira*
Otu27	*Clostridium_Candidatus_Arthromitus*
Otu28	*Akkermansia*
Otu29	*Parabacteroides*
Otu30	*Mucispirillum*
Otu31	*Hydrogenoanaerobacterium*
Otu32	*Roseburia*
Otu33	*Ruminococcus*
Otu34	*Candidate_division_TM7*
Otu35	*Lachnospira*
Otu36	*Lactobacillaceae_unclassified*
Otu37	*Enterococcus*
Otu38	*Parasutterella*
Otu39	*Pseudomonas*
Otu40	*Porphyromonadaceae_unclassified*

OTU	Taxonomy
Otu41	*Alcaligenes*
Otu42	*Weissella*
Otu43	*Robinsoniella*
Otu44	*Acinetobacter*
Otu45	*Erysipelotrichaceae_Incertae_Sedis*
Otu46	*Lactobacillales_unclassified*
Otu47	*Olsenella*
Otu48	*Bifidobacterium*
Otu49	*Streptococcus*
Otu50	*Clostridia_unclassified*
Otu51	*Clostridium_unclassified*
Otu52	*Escherichia*
Otu53	*Staphylococcus*
Otu54	*Desulfovibrio*
Otu55	*Mollicutes_unclassified*
Otu56	*Actinobacteria_unclassified*
Otu57	*Eubacterium*
Otu58	*Turicibacter*
Otu59	*Peptococcaceae*

Figure 5

Complex microbial interaction networks based on 177,147 simulations. Each node represents a genus. Node color represents degree, node size represents betweenness centrality, and text size represents closeness centrality. The color of the edge represents the strength of the interaction between two nodes. A) Microbial interaction network of Sham group; n=3. B) Microbial interaction network of SNI group; n=3.

Supplementary Files

This is a list of supplementary files associated with this preprint. Click to download.

- SupplementarymaterialsDaryiWangrevised.docx
- NC3RsARRIVEGuidelinesChecklist2014DaryiWang.docx